Journal of Physical Science, Vol. 28(Supp. 1), 201–213, 2017

Thickness Effect on the Morphology and Permeability of CO_2/N_2 Gases in Asymmetric Polyetherimide Membrane

Abdul Latif Ahmad, [1*] Salaudeen Yusuf Olatunji[1] and Zeinab Abbas Jawad[2]

[1]School of Chemical Engineering, Universiti Sains Malaysia,
Engineering Campus, 14300 Nibong Tebal, Pulau Pinang, Malaysia
[2]School of Engineering and Science, Chemical Engineering Department,
Curtin University Sarawak, CDT 250, 98009 Miri, Sarawak, Malaysia

[*]Corresponding author: chlatif@usm.my

Published online: 15 February 2017

To cite this article: Ahmad, A. L., Olatunji, S. Y. & Jawad, Z. A. (2017). Thickness effect on the morphology and permeability of CO_2/N_2 gases in asymmetric polyetherimide membrane. *J. Phys. Sci.*, 28(Supp. 1), 201–213, https://doi.org/10.21315/jps2017.28.s1.13

To link to this article: https://doi.org/10.21315/jps2017.28.s1.13

ABSTRACT: *The effect of membrane thickness on the morphology and performance of polyetherimide (PEI) flat sheet membranes for gas separation has been investigated. An asymmetric PEI flat sheet membrane was fabricated using phase inversion with N-methyl-2-pyrrolidone (NMP) and water-isopropanol as solvent and coagulant, respectively. Scanning electron microscopy (SEM) was used to analyse the morphology of the prepared membrane. The results showed that the membrane with high casting thickness of 300 µm yielded a lower permeability compared to the fabricated membrane with lower casting thickness at 1 bar and 25°C for pure carbon dioxide (CO_2) and nitrogen (N_2) as test gas. It was found that the permeability strongly depended on the cast solution thickness. It was also found out that the macrovoid became open and appeared larger as the casting thickness increased.*

Keywords: PEI membrane, asymmetric, CO_2/N_2 separation, isopropanol, permeability

1. INTRODUCTION

The use of membranes for gas separation has been recognised for many decades since the first successful development of integrally skinned asymmetric membrane prepared by Loeb and Sourirajan in 1960.[1] These membranes were limited to a certain degree of perfection and thickness of the selective layer affixed on the porous support in form of composite membrane. Besides the Robeson trade-off,

there is usually another trade-off relationship between permeance (related to the skin thickness) and selectivity (related to the integrity of the skin). The membrane sub-layer serves as a mechanical support for the skin, with negligible effect on separation. Macrovoids can usually be observed in asymmetric membrane fabricated by phase inversion process. In high-pressure operation during gas separation, the presence of macrovoid is not generally favorable because this usually leads to mechanical weakness.[2,3] The performance of membrane-based gas separation process strongly depends on permeability and selectivity of the membrane. A membrane with higher permeability yields higher productivity and low capital cost, whereas membrane with higher selectivity leads to more efficient separation, high recovery as well as low power cost. The membrane that simultaneously possesses a high value of selectivity and permeability would lead to the most economical gas separation process.[4]

Phase inversion process induced by immersion precipitation is a well-known technique to fabricate asymmetric membranes. During immersion precipitation, the substrate in the coagulation bath and the solvent in the casting solution film are exchanged with non-solvent (NS) in precipitation media which results in phase separation. This process yields the formation of asymmetric membrane with a dense top layer as well as a porous sub-layer containing macrovoids, pores and micropores. The sub-layer formation is controlled by numerous variables in the polymer dope solutions such as composition, coagulant temperature and organic/inorganic additives. To attain a desired membrane morphology and performance, the phase inversion process must be carefully controlled.[5] The exchange in solvent and non-solvent may result in instability within the membrane-forming system which is followed by a phase separation to make polymer-rich and polymer-lean phases that can produce the matrix of the membrane and pores, respectively.[6–10] The liquid–liquid demixing by nucleation and growth of a polymer-lean phase is responsible for generating porous morphology.[9]

CO_2/N_2 separation is one of the most interesting processes in the energy industry because of gas recovery and decreasing flaring emissions. Membrane separation is one of the new perspective methods for such applications. This method has more advantages than other traditional gas separation techniques such as cryogenic distillation and pressure swing adsorption. These include energy saving, easy installation, operation as well as maintenance, modular and low space requirements, and environmentally friendly.[11] The polymeric membrane should be able to offer significant improvements in CO_2 permeability and selectivity with excellent thermal and chemical stability, resistance to plasticisation, resistance to aging, and ease of scale-up in order to be commercially competitive.[12]

Commercially available polyetherimide (PEI) has several important advantages as a membrane material. This polymer has good chemical and thermal stability. The aromatic imide units provide stiffness and heat resistance, while the swivel groups such as -O and -$C(CH3)_2$ form flexible macromolecular chains that allow for good processability.[13] A study by Wang et al.[13] on gas permeation of the PEI dense films revealed that PEI exhibits an impressively high selectivity for many important gas pairs especially He and H_2 separation from other gasses. In 2013, Shamsabadi et al.[14] prepared flat sheet asymmetric PEI membrane for the separation of H_2 from CH_4 which resulted in an ideal selectivity of 27.8. Meanwhile, Saedi et al.[15] fabricated asymmetric flat sheet polyethersulfone (PES) membrane for separation of CO_2 from CH_4 using PEI as a polymeric additive which led to CO_2 permeance of 11.1 at 5 bars. Ren et al.[7] also prepared the PEI flat sheet membrane with N-methyl-2-pyrrolidone (NMP)/non-solvent system. In their study, they investigated the influence of various non-solvents on the membrane morphology. Kurdi and Tremblay[16] produced a defect-free PEI asymmetric flat sheet membrane for the separation of oxygen from nitrogen using $LiNO_3$ and isopropanol as dual bath coagulation method. Simons et al.[17] investigated CO_2 and CH_4 sorption as well as transport behaviour using the PEI membrane which produced CO_2 permeability of 1.4 at 5 bars. In 1987, Pinnau et al.[18] prepared PEI flat-sheet asymmetric membranes for CO_2/CH_4 separation using a halogenated hydro-carbon as solvent and reported a selectivity of about 30–40.

In this study, we fabricated structural transition of asymmetric PEI flat sheet membranes prepared with different thicknesses of cast solution. The morphology and the performances for CO_2/N_2 separation of the produced membrane were investigated.

2. EXPERIMENTAL

2.1 Materials

Polyetherimide (PEI, Ultem®) was purchased from General Electric Plastics (Malaysia). Figure 1 represents the molecular structure of the used polyetherimide. Table 1 shows the physical properties of the PEI. Also, isopropanol, anhydrous 1-methyl-2-pyrrolidinone (NMP) (EMPLURA1, 99.5%, water < 0.1%) were supplied by Merck, Malaysia. CO_2 (99.9%) and N_2 (99.9%) were supplied by Technical Gas Services, Malaysia.

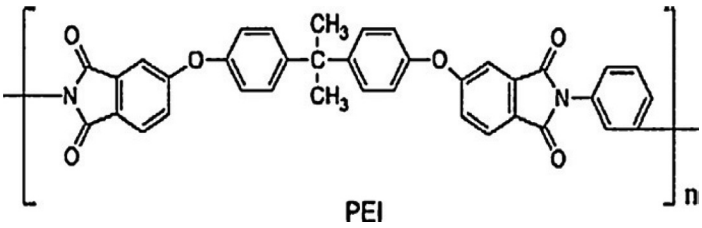

Figure 1: The molecular structure of used PEI where *n* represents the degree of polymerisation.

Table 1: The physical properties of polyetherimide (PEI).

Properties	Units	Values
Molecular weight	kg $Kmol^{-1}$	30,000
Density	kg/m^3	1270
Water absorption	mg	20/41
After 24 h/996 h immersion in water of 23°C		
Melting point	°C	219
Glass transition temperature	°C	206
Thermal conductivity at 23°C	W/ (m.K)	0.22
Specific heat	$kJ.kg^{-1}. K^{-1}$	2.0
Upper working temperature	°C	170–200
Elongation at break	%	15
Compressive strength	MPa	140
Tensile strength	MPa	85

2.2 Fabrication of PEI Asymmetric Flat Sheet Membrane

PEI was dried in a vacuum oven at 110°C overnight in order to remove any trace of adsorbed humidity. The desired polymer solution (w/w) was prepared by dissolving a certain weight of PEI in a pre-determined weight of NMP in a closed glass jar. A stirring speed of 400 rpm at 60°C was applied for efficient mixing for 24 h until a clear yellowish uniform viscous solution was achieved and left overnight. Then the solution was degassed for 30 min in order to remove the air bubbles from the solution. After the degassing process, the polymer solution was cast on a glass plate with a different thickness of 150–300 µm with the aid of casting knife by a motorised film applicator (Elcometer 4340, Dutech Instruments Malaysia). The cast film along with the glass plate were immediately immersed in a water–isopropanol (4:1 of water: isopropanol) bath to accomplish the phase

inversion for 5 min, followed by immersing the membrane in distilled water for 24 h. Subsequently, the membrane was placed in between two dried glasses filled with sheets of filter paper and dried for 24 h at room temperature. Finally, the PEI membrane was dried in an oven at 70°C ± 2°C for 12 h for the complete removal of solvents and adsorbed humidity. The dope composition was represented in Table 2.

Table 2: The composition of the polymer solution.

Solution no	PEI	NMP	Coagulant (water: isopropanol)	Casting thickness
N-1	25	75	4:1	150
N-2	25	75	4:1	250
N-3	25	75	4:1	300

2.3 Gas Permeation Test

A gas permeation experiment was performed using an assembled setup as shown in Figure 2. A cross-flow membrane cell made from stainless steel was used to perform the experiments. The cell consists of two detachable circular compartments clamped together by six screws. The upper part was connected to the feed and the retentate streams. The permeate streams were exhausting from the lower part. Circular membrane discs with effective permeation area of 7.0 cm^2 were used. The pressure-normalised fluxes of the fabricated flat sheet membranes were measured for pure CO_2 and N_2 at 25°C and 1 bar. The feed gas was supplied to the shell side of the module. The standard permeate volumetric flow rate at atmospheric conditions was measured by a soap bubble flow meter. Each set of data represents an average of 6 replicates. The pressure-normalised flux (permeance) which flows through the membranes was calculated using Equation 1:

$$\left(\frac{p}{l}\right) = \frac{Q}{A\Delta P} \tag{1}$$

where Q is the measured volumetric flow rate (at standard pressure and temperature) of the permeated gas (cm^3 (STP)/s), p is permeance, l is membrane thickness (cm), A is the effective membrane area (cm^2) and ΔP is the pressure difference across the membrane (cmHg). The common unit of permeance is GPU where GPU is equal to cm^3 (STP)/cm^2 s cmHg. Also, the ideal gas separation factor (α) can be calculated using Equation 2:

$$\alpha_{CO_2}/N_2 = \frac{PCO_2/l}{PN_2/l} \tag{2}$$

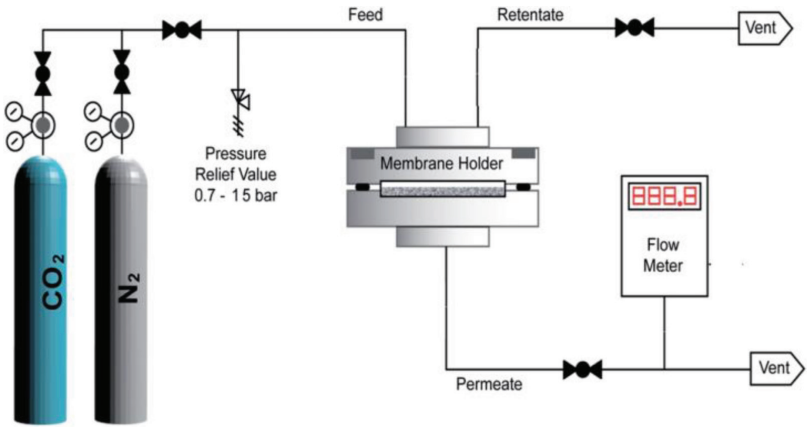

Figure 2: Schematic diagram of gas permeation set up.

2.4 Characterisation of Flat Sheet Polyetherimide Membrane

The morphology of fabricated flat sheet membranes was investigated using scanning electron microscope (SEM) (TM 3000 Hitachi, High-Tech TOKYO) with an accelerating voltage of 25.0 kV. Prior to scanning, small pieces of the membrane samples were immersed into liquid nitrogen carefully for a minimum of 120 s. Then, it was fractured to obtain a clear cross section. After drying, the fractured membrane sheet was placed on a disc for sputtering with a thin film of platinum prior to SEM testing.

3. RESULTS AND DISCUSSION

3.1 Effect of Thickness on Membrane Structure

Figure 3 shows the SEM micrograph for the cross-sectional morphologies of 25 wt.% PEI membrane fabricated under different casting thicknesses. The presence of densed skin layer with porous substructure was observed from the three membranes cast with a thickness of 150, 250 and 350 µm (Figure 3 (a), (b) and (c)). The skin layer (selective layer) of these three membranes increases as the casting thickness increases. The thickness of these skin layers was measured to be approximately 7.268 µm, 18.853 µm, and 26.330 µm, respectively. On the other hand, the sub-layer of these three membranes has a finger-like macrovoid but it was observed that the macrovoid of the membrane cast with a thickness of 300 µm is significantly larger than the membranes cast with lower thickness. This

reveals that macrovoid size increases with membrane casting thickness. Li et al.[19] reported similar behaviour which was further attributed to the existence of critical structure-transition thickness. The transition was initiated with a fully sponge-like structure forming in the first region, followed by some fluctuations into the finger-like structure and ended with the fully formed finger-like structure as the thickness increased.

Mulder[2] described the macrovoid formation mechanism during membrane precipitation as a phenomenon that originates from the formation of nuclei at the polymer lean region which is near to the membrane surface. Due to further diffusion and displacement of the solvent/non-solvent pair, the macrovoid becomes larger. The Monte Carlo diffusion by Termonia also supported that the macrovoid initiation was through non-solvent penetration via skin defects and the faster exchange rate between solvent and non-solvent aided the growth.[20] For lower membrane thickness (i.e., 150 μm), the presence of the thin layer of macrovoid was due to insufficient space for the membrane to be formed between the film and the bottom surface. However, the formation of finger-like macrovoid exhibited in thicker membrane thickness was as a result of the non-solvent inflow which dominated the exchange rate during the membrane precipitation.

Zhang et al.[21] reported that finger-like macovoid of cellulose acetate membrane prepared disappeared as the thickness is lowered down when the critical thickness is at 150 μm. From Figure 3(a), it was observed that the macrovoid formed at the skin layer of the membrane prepared with lower casting thickness of 150 μm is in compact that it cannot be easily seen, unlike the other two membranes prepared from higher casting thicknesses of 250 and 300 μm in Figure 3(b) and 3(c) respectively, where the macrovoid at the skin layer becomes open and larger. This can be attributed to the fact that the speed of demixing point in skin layers is extremely faster because of the higher concentration gradient in such thickness. Similar reason was reported by Safi et al.[22] that the thickness of the membrane is in relation to the macrovoid. In their study, they concluded that finger-like structures and the pores were far away from top layer in a lower thickness of cast solution, while at higher thickness values, they existed just beneath the top layer.

Tsay and McHugh[23] explained that an increase in the skin layer thickness was a result of the decrease in asymmetric porous sub-layer due to increase in the membrane thickness. This reason was attributed to the sponge-like formation which was established as can be seen in the membrane prepared with 250 and 300 μm. Besides, the macrovoid-free structure could prevent the mechanically weak point in the membrane structures and this can be attained below the critical thickness.[19,24]

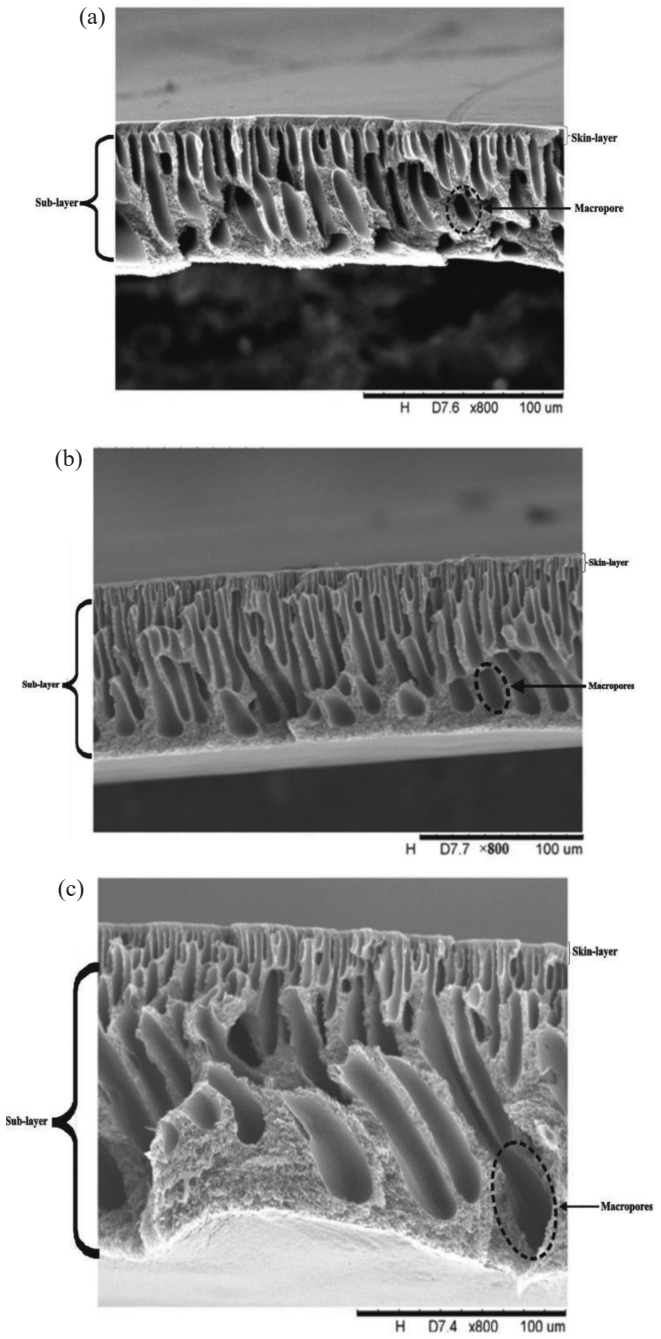

Figure 3: SEM images of polymer concentration prepared from 25 wt.% but with different thickness (a) 150 µm (b) 250µm (c) 300 µm.

3.2 Effect of Thickness on Gas Permeation Performance

As can be seen from the results presented in Table 3, the membrane with a thickness of 150 μm in N-1 has a permeability of 10.365 Barrer for CO_2 gas with a separation factor of 1.7. However, permeability was drastically reduced to 2.588 Barrer for CO_2 with thickness increment to 300 μm in N-3. Meanwhile, the selectivity increased to 2.6 with a thickness of 300 μm and this was due to the thickness of the selective layer and the formation of the most sponge-like structure at the sublayer of this membrane. From Table 4, one can see that the permeability of CO_2 is encouraged when compared to other works. This result was in tandem with the report by Firpo et al.[25] that the permeability shows a strong decrease with increase in thickness but the selectivity does not change significantly in its value. Pakizeh et al.[26] reported that CO_2 molecules are absorbed at a high level on the skin layer surface and can then diffuse through the dense layer of the membrane. Therefore, the CO_2 permeability is governed by the skin layer thickness.

Table 3: Effect of casting thickness on membrane permeability and selectivity.

Membrane sample	CO_2 permeability (Barrer)	N_2 permeability (Barrer)	CO_2/N_2 selectivity
N-1	10.365	5.956	1.740
N-2	4.382	1.770	2.476
N-3	2.588	1.012	2.559

Table 4: Correlation of permeability and selectivity with other polymer.

Polymers	CO_2 permeability (Barrer)	N_2 permeability (Barrer)	Selectivity	References
PEI + Zeolite	0.21	0.0067	31	30
PEI/NMP/Coagulant	10.365	5.956	1.740	This work

However, when the thickness of the densed skin layer decreases, the permeability of CO_2 increases. As can be seen from the permeability results in Table 3, the permeability of CO_2 is of higher values compared to that of N_2 gas. This may be due to two mechanisms. Firstly, the high potential of CO_2 to diffuse through the polymer matrix due to its small kinetic diameter (3.3Å) than N_2 (3.64Å).[27] Secondly, a quadrupolar moment of CO_2 in combination with glassy nature of PEI increases its permeability for CO_2 than N_2. Indeed, CO_2 is a condensable and interactive gas which can interact with the polymeric chains and the available functional groups. This leads to a high solubility for CO_2, and consequently, being more permeable than N_2 gas. Besides, the lower permeability of N_2 might be due

to slow diffusivity resulting from the larger kinetic diameter and solubility in the PEI polymer.[28] It was also reported by Alsari et al.[29] in their study, where they laid much emphasis on the importance of membrane thickness to the separation of gas as the thickness increased, the permeability drastically reduced.

In summary, the accumulated data gives an insight that membrane thickness was directly related to the permeability of gas. It was observed that a thick layer was formed in membrane fabricated with a thickness of 300 μm which caused the lower permeability and an improvement in the selectivity of the gas. This signifies that the higher the membrane thickness, the lower the permeability is with no significant changes in the separation factor.

4. CONCLUSION

Asymmetric PEI membranes were successfully fabricated through phase inversion process for removal of CO_2 in single gas permeation test. The membrane casting thickness was explored and has been identified as one of the parameters in controlling the final morphologies and performances of the prepared membranes. A study on the casting membrane thickness was carried out and its correlation was attributed to the formation of macrovoid in the structure and permeability in the gas permeation test. SEM images of the cross-sectioned membrane with varied casting thickness (150, 250 and 300 μm) revealed that the macovoid is easily formed near the skin layer in the membrane with a high thickness of 300 μm which caused the low permeability.

As observed, gas permeation properties of the selective layers with different thickness defined that the permeability of the gases decreases upon the increase in the film thickness. However, the CO_2/N_2 selectivities remained insignificantly changed. Nevertheless, a trade-off relationship between permeability and selectivity was normally observed in the manipulation of the asymmetric membrane using thickness as an affecting parameter.

5. ACKNOWLEDGEMENTS

The authors would like to acknowledge and thank the research grant 203. PJKIMIA.6071334 provided by Universiti Sains Malaysia that made this study successful.

6. REFERENCES

1. Loeb, S. (1963). Sea water demineralization by means of a semipermeable membrane. Progress report, 1 July 1962–31 December 1962. Department of Engineering, University of California, Los Angeles, United States.
2. Mulder, J. (2012). *Basic principles of membrane technology*. Amsterdam: Springer Science & Business Media.
3. Smolders, C. A. et al. (1992). Microstructures in phase-inversion membranes. Part 1. Formation of macrovoids. *J. Membr. Sci.*, 73, 259–275, http://dx.doi.org/10.1016/0376-7388(92)80134-6.
4. Ismail, A. F. & Lai, P. Y. (2003). Effects of phase inversion and rheological factors on formation of defect-free and ultrathin-skinned asymmetric polysulfone membranes for gas separation. *Sep. Purif. Technol.*, 33, 127–143, http://dx.doi.org/10.1016/S1383-5866(02)00201-0.
5. Albrecht, W. et al. (2001). Formation of hollow fiber membranes from poly(ether imide) at wet phase inversion using binary mixtures of solvents for the preparation of the dope. *J. Membr. Sci.,* 192, 217–230, http://dx.doi.org/10.1016/S0376-7388(01)00504-X.
6. Azari, S., Karimi, M. & Kish, M. (2010). Structural properties of the poly (acrylonitrile) membrane prepared with different cast thicknesses. *Ind. Eng. Chem. Res.*, 49, 2442–2448, https://doi.org/10.1021/ie900952v.
7. Ren, J., Zhou, J. & Deng, M. (2010). Morphology transition of asymmetric polyetherimide flat sheet membranes with different thickness by wet phase-inversion process. *Sep. Purif. Technol.*, 74, 119–129, https://doi.org/10.1016/j.seppur.2010.05.014.
8. Stropnik, C., Germic, L. & Zerjal, B. (1996). Morphology variety and formation mechanisms of polymeric membranes prepared by wet phase inversion. *J. Appl. Polym. Sci.*, 61, 1821–1830, https://doi.org/10.1002/(SICI)1097-4628(19960906)61:10%3C1821::AID-APP24%3E3.0.CO;2-3.
9. Van de Witte, P. et al. (1996). Phase separation processes in polymer solutions in relation to membrane formation. *J. Membr. Sci.*, 117, 1–31, https://doi.org/10.1016/0376-7388(96)00088-9.
10. Vogrin, N. et al. (2002). The wet phase separation: The effect of cast solution thickness on the appearance of macrovoids in the membrane forming ternary cellulose acetate/acetone/water system. *J. Membr. Sci.*, 207, 139–141, https://doi.org/10.1016/S0376-7388(02)00119-9.
11. Baker, R. W. (2002). Future directions of membrane gas separation technology. *Ind. Eng. Chem. Res.*, 41, 1393–1411, https://doi.org/10.1021/ie0108088.

12. Iarikov, D. D. & Oyama, S. T. (2011). Review of CO2/CH4 separation membranes. *Membr. Sci. Technol.*, 14, 91–115, https://doi.org/10.1016/B978-0-444-53728-7.00005-7.
13. Wang, D., Li, K. & Teo, W. (1998). Preparation and characterization of polyetherimide asymmetric hollow fiber membranes for gas separation. *J. Membr. Sci.*, 138, 193–201, https://doi.org/10.1016/S0376-7388(97)00229-9.
14. Shamsabadi, A. A. et al. (2013). Separation of hydrogen from methane by asymmetric PEI membranes. *J. Ind. Eng. Chem.*, 19, 1680–1688, https://doi.org/10.1016/j.jiec.2013.02.006.
15. Saedi, S., Madaeni, S. S. & Shamsabadi, A. A. (2014). Fabrication of asymmetric polyethersulfone membranes for separation of carbon dioxide from methane using polyetherimide as polymeric additive. *Chem. Eng. Res. Des.*, 92, 2431–2438, https://doi.org/10.1016/j.cherd.2014.02.010.
16. Kurdi, J. & Tremblay, A. (1999). Preparation of defect-free asymmetric membranes for gas separations. *J. Appl. Polym. Sci.*, 73, 1471–1482, https://doi.org/10.1002/(SICI)1097-4628(19990822)73:8%3C1471::AID-APP16%3E3.0.CO;2-G.
17. Simons, K. et al. (2010). CO_2 sorption and transport behavior of ODPA-based polyetherimide polymer films. *Polym.*, 51, 3907–3917, https://doi.org/10.1016/j.polymer.2010.06.031.
18. Pinnau, I., Wind, J. & Peinemann, K. V. (1990). Ultrathin multicomponent poly (ether sulfone) membranes for gas separation made by dry/wet phase inversion. *Ind. Eng. Chem. Res.*, 29, 2028–2032, https://doi.org/10.1021/ie00106a009.
19. Li, D. et al. (2004). Thickness dependence of macrovoid evolution in wet phase-inversion asymmetric membranes. *Ind. Eng. Chem. Res.*, 43, 1553–1556, https://doi.org/10.1021/ie034264g.
20. Termonia, Y. (1995). Fundamentals of polymer coagulation. *J. Polym. Sci. B*, 33, 279–288, https://doi.org/10.1002/polb.1995.090330213.
21. Zhang, S. et al. (2011). Molecular design of the cellulose ester-based forward osmosis membranes for desalination. *Chem. Eng. Sci.*, 66, 2008–2018, https://doi.org/10.1016/j.ces.2011.02.002.
22. Safi, R., Karimi, M. & Madhi, A. (2015). Structural transition of asymmetric poly (ether imide) membrane prepared by wet phase inversion. *Polym. Bull.*, 72, 1763–1774, https://doi.org/10.1007/s00289-015-1369-5.
23. Tsay, C. S. & McHugh, A. (1991). The combined effects of evaporation and quench steps on asymmetric membrane formation by phase inversion. *J. Polym. Sci. B*, 29, 1261–127, https://doi.org/10.1002/polb.1991.0902910100.

24. Peng, N., Chung, T.-S. & Wang, K. Y. (2008). Macrovoid evolution and critical factors to form macrovoid-free hollow fiber membranes. *J. Membr. Sci.*, 318, 363–372, https://doi.org/10.1016/j.memsci.2008.02.063.
25. Firpo, G. et al. (2015). Permeability thickness dependence of polydimethylsiloxane (PDMS) membranes. *J. Membr. Sci.*, 481, 1–8, https://doi.org/10.1016/j.memsci.2014.12.043.
26. Pakizeh, M. et al. (2013). Modification of PSf membrane nanostructure using different fabrication parameters and investigation of the CO_2 separation properties of PDMS-coated PSf composite membranes. *Braz. J. Chem. Eng.*, 30, 345–354, https://doi.org/10.1590/S0104-66322013000200012.
27. Murali, R. S. et al. (2014). Mixed matrix membranes of Pebax-1657 loaded with 4A zeolite for gaseous separations. *Sep. Purif. Technol.*, 129, 1–8, https://doi.org/10.1016/j.seppur.2014.03.017.
28. Sadeghi, M. et al. (2008). Gas permeation properties of ethylene vinyl acetate–silica nanocomposite membranes. *J. Membr. Sci.*, 322, 423–428, https://doi.org/10.1016/j.memsci.2008.05.077.
29. Alsari, A., Kruczek, B. & Matsuura, T. (2007). Effect of pressure and membrane thickness on the permeability of gases in dense polyphenylene oxide (PPO) membranes: Thermodynamic interpretation. *Sep. Sci. Technol.*, 42, 2143–2155, https://doi.org/10.1080/01496390701446266.
30. Husain, S. & Koros, W. J. (2007). Mixed matrix hollow fiber membranes made with modified HSSZ-13 zeolite in polyetherimide polymer matrix for gas separation. *J, Membr. Sci.*, 288, 195–207, https://doi.org/10.1016/j.memsci.2006.11.016.